Tsiavos, A., Alexander, N., Diambra, A., Ibraim, E., Vardanega, P., Gonzalez-Buelga, A., & Sextos, A. (2019). A sand-rubber deformable granular layer as a low-cost seismic isolation strategy in developing countries: Experimental investigation. *Soil Dynamics and Earthquake Engineering*, *125*, [105731]. https://doi.org/10.1016/j.soildyn.2019.105731

Soil Dynamics and Earthquake Engineering 125 (2019) 105731

Contents lists available at ScienceDirect

Soil Dynamics and Earthquake Engineering

journal homepage: www.elsevier.com/locate/soildyn

A sand-rubber deformable granular layer as a low-cost seismic isolation strategy in developing countries: Experimental investigation

Anastasios Tsiavos[a,*], Nicholas A. Alexander[b], Andrea Diambra[c], Erdin Ibraim[d], Paul J. Vardanega[e], Alicia Gonzalez-Buelga[f], Anastasios Sextos[g]

[a] Department of Civil Engineering, University of Bristol, UK
[b] Department of Civil Engineering, University of Bristol, UK
[c] Department of Civil Engineering, University of Bristol, UK
[d] Department of Civil Engineering, University of Bristol, UK
[e] Department of Civil Engineering, University of Bristol, UK
[f] Department of Civil Engineering, University of Bristol, UK
[g] Department of Civil Engineering, University of Bristol, UK & Aristotle University of Thessaloniki, Greece

ARTICLE INFO

Keywords:
Sand-rubber layer
Seismic isolation
Developing countries

ABSTRACT

This paper presents experimental investigations on the feasibility of using a sand-rubber deformable granular layer as a low-cost seismic isolation strategy for developing countries. The mechanical characteristics of a potential failure mechanism inside the sand-rubber layer are investigated. Direct shear testing is performed to quantify the angle of friction of three different sand-rubber mixtures subjected to different vertical stress levels. The experimentally derived mechanical characteristics are compared to the corresponding values for pure rubber and pure sand samples. The frictional characteristics of sliding between a sand-rubber layer and a timber interface are identified. Direct shear testing is performed to quantify the quasi-static friction of the same sand-rubber mixtures against a timber interface, that is part of the foundation casting, subjected to alternative vertical stresses. The effect of the shear rate and the saturation of the sand-rubber mixture on the aforementioned mechanical characteristics is presented. A uniaxial shaking table experimental setup is used for the investigation of the dynamics of a rigid sliding block and the quantification of the kinetic friction of different sliding interfaces against two different sand-rubber mixtures for two different sand-rubber layer heights. The rigid sliding block designed to slide against the sand-rubber layer is subjected to both a harmonic ramp loading and earthquake ground motion excitation. The design outcome of this static and dynamic experimental investigation is the determination of the optimum grain size ratio and the height of the sand-rubber layer, that corresponds to the lower (and more favourable from a seismic isolation view point) friction coefficient between the sand-rubber layer and the foundation. The quantification of these fundamental parameters paves the way for a holistic design of a response modification strategy for mitigating seismic damage in developing countries.

1. Introduction

Seismic isolation is extensively used as an effective response modification strategy, leading to the reduction of seismic damage of numerous structures located in developed countries [1–3]. The limitations of seismic isolation are (i) significant up-front cost, (ii) the potentially large isolation layer drift levels and (iii) the fact that its efficiency is better suited to low period systems. An extension of this response modification strategy to low income (i.e., developing) countries [4,5] would require a significant reduction of the installation and maintenance cost of the isolation systems. Additionally, it would be very helpful if the highly-engineered friction pendulum and rubber isolation systems could be replaced with an alternative low-cost system that makes use of materials that are locally available and cost-effective in these regions.

The goal of this paper is to investigate experimentally the feasibility of the design of a sliding layer consisting of a deformable sand-rubber granular mixture as a seismic isolation strategy for low-rise, small footprint buildings in developing countries. The idea is that the fine sand can be locally obtained and the rubber can be sustainably sourced from recycled vehicle tyres. The design of such a low-cost seismic isolation strategy consisting of these locally available materials is an issue

* Corresponding author.
E-mail address: a.tsiavos@bristol.ac.uk (A. Tsiavos).

https://doi.org/10.1016/j.soildyn.2019.105731
Received 22 March 2019; Received in revised form 17 May 2019; Accepted 17 June 2019

of paramount importance for the seismic damage mitigation and the resilience of the communities in these countries.

Several researchers have investigated design alternatives aiming at the reduction of the construction cost of seismic isolators. Kelly [6] conducted an analytical and experimental study on the feasibility of the use of fiber reinforcement for the design of low-cost elastomeric isolators for seismic damage mitigation in developing countries. Kelly and Konstantinidis [7] explored the possibility of using an unbonded bridge bearing to decrease the construction cost of rubber seismic isolators. Castaldo and Ripani [8] quantified the influence of the soil deformability on the optimal frictional characteristics of seismically isolated bridges, aiming at an optimization of the construction cost of these structures. Banović et al. [9] performed shaking table experimental investigations on the use of a stone pebble layer as a low-cost seismic isolation strategy based on a sliding mechanism.

The soil deformability and its potential use as an economic design alternative for seismic isolation of structures has been extensively studied in the past. Trifunac and Todorovska [10] and Trifunac [11] have studied the nonlinear soil response as a natural passive isolation mechanism. Gazetas et al. [12] and Anastasopoulos and Kontoroupi [13] have quantified the nonlinear rocking stiffness of foundations and explored the potential use of soil failure below the foundation of structures for seismic isolation purposes. The challenge associated, however, with the utilization of the nonlinear soil response for seismic isolation is the residual differential settlement in the soil after the occurrence of a possible deleterious ground motion excitation. Self-centering mechanisms or measures for the realignment of the structure are usually required to restore the functionality of the structure after the occurrence of the ground motion excitation.

In light of these challenges, different approaches have been proposed towards the improvement of the mechanical characteristics of sands through their mixture with rubber particles. The use of rubber particles from scrap tyres has significant environmental advantages and is growing in civil engineering applications (ASTM D627017 [14]) due to the high amount of the produced scrap tyres worldwide. Ahmed [15], Tweedie et al. [16] and Hazarika et al. [17,18] observed that using shredded, scrap tyres in lightweight backfills decreases the settlement of retaining structures. Edil and Bosscher [19], Masad et al. [20], Foose et al. [21], Lee et al. [22] and Kim and Santamarina [23] determined the fundamental parameters that influence the mechanical response and the deformability of granulated sand-rubber mixtures. These parameters are (i) the ratio of mean particle grain sizes between rubber ($D_{50,r}$) and sand grains ($D_{50,s}$) and (ii) the volume fraction of rubber (F_R) in the mixture. Lopera Perez et al. [24,25] determined through discrete simulations the fundamental load transfer mechanisms between sand-sand, sand-rubber and rubber-rubber contacts which control the strength and instability of sand-rubber mixtures with different mean grain size ratios $D_{50,r}/D_{50,s}$. These studies showed a significant reduction of the contribution of the sand-sand contacts to the behaviour of the mixture and increased rubber-like behaviour for higher rubber fraction levels. Rouhanifar and Ibraim [26] have shown that increasing the rubber fraction in a granular sand-rubber mixture above 30% leads to a decrease of 15% in the mobilized peak and large-strain angle of friction of the mixture and makes the mechanical response of the mixture dominated by its rubber particles.

The dynamic characteristics of sand-rubber mixtures have been determined analytically [27,28] and experimentally through shaking table testing [29,30]. Common theme across the aforementioned studies is the strain-dependent dynamic behaviour of sand-rubber mixtures under cyclic and dynamic loads. The small-strain damping ratio of soil-rubber mixtures is higher than the ratio of pure granular soils and increases for higher rubber fractions [31] and increasing shearing strain amplitudes [27,28].

The attractive static and dynamic properties along with the environmental advantages, the low-cost and the material availability of sand-rubber mixtures facilitate their use for seismic isolation of structures in developing countries. Tsang [32,33] and Mavronicola et al. [34] presented a numerical investigation of the feasibility of the use of sand-rubber mixtures for seismic isolation of structures in developing countries, concluding that the use of this seismic isolation strategy can reduce substantially not only the horizontal but also the vertical ground motion acceleration response of structures subjected to earthquake ground motion excitation. Brunet et al. [35] and Pitilakis et al. [36] quantified numerically the effectiveness of a seismic isolation strategy consisting of sand-rubber mixtures for different sand-rubber layer thicknesses and building heights. Tsang and Pitilakis [37] investigated numerically the elastic rocking behaviour of structures founded on a sand-rubber layer as an alternative seismic isolation mechanism.

However, these investigations of different geotechnical seismic isolation (GSI) systems as defined by Tsang [38] did not include any experimental verification and have not focused on the exact specification of the optimal grain size ratio and the mechanical and geometrical characteristics of a sand-rubber mixture towards the minimization of the seismic accelerations and forces acting on the seismically isolated structure.

Along these lines, the goal of this study is to determine experimentally the optimal grain size ratio of a sand-rubber mixture and the optimal sliding interface between the mixture and the seismically isolated structure, that lead to a balanced response between the desirable sliding and bearing capacity of the foundation thus laying the basis for a holistic design of a response modification strategy for seismic damage mitigation in developing countries. The above experimental campaign, based on direct shear and shaking table dynamic testing of different sand-rubber mixtures, is performed in the Geotechnics Laboratory and the Dynamics Laboratory of the University of Bristol.

2. Experimental procedure of direct shear testing of sand-rubber mixtures

Several researchers have amended the conventional direct shear apparatus to restrain the upper frame and the load pad rotation (e.g. Jewell and Wroth [39]; Shibuya et al. [40]; Lings and Dietz [41]). The modified direct shear apparatus proposed by Lings and Dietz [41] was used in this study for the direct shear testing and the quantification of the friction angle of different sand-rubber mixtures (Fig. 1). The shear load is applied using two 'wings' connected with the upper frame of the apparatus. This arrangement enables the application of the load near the centre of the shear box, the reduction of the rotations comparing to the conventional apparatus, the unrestricted dilation of the sample and facilitates reverse shear testing. This apparatus has already been used for earthquake engineering purposes: O'Rourke [42] used this apparatus for the seismic assessment of water supply systems in San Francisco and Los Angeles and recommended its use for direct shear testing of soil samples.

The friction angle of three different sand-rubber mixtures was

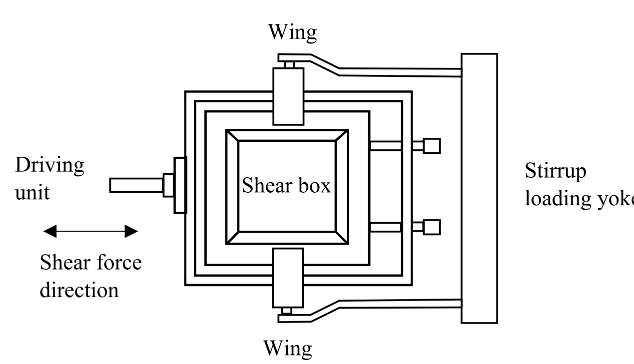

Fig. 1. Overview of the modified direct shear apparatus proposed by Lings and Dietz [41].

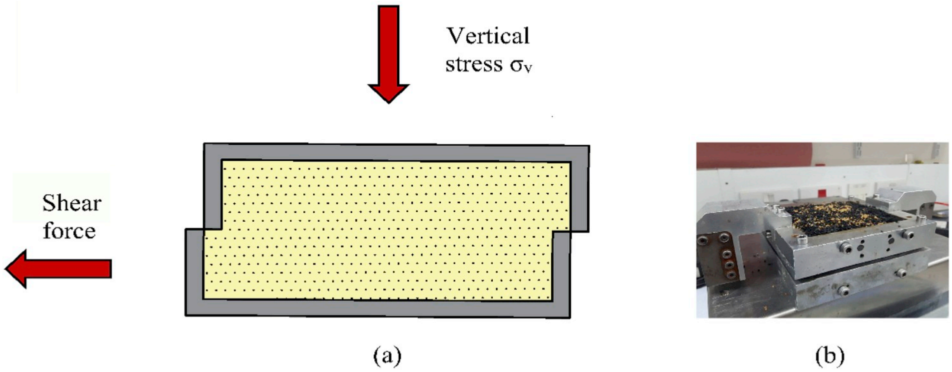

Fig. 2. (a) Schematic representation and (b) Picture of direct shear testing of a sand-rubber mixture.

Table 1
Mean grain sizes and relative grain size distribution ratios for three different sand-rubber mixtures.

	Rubber		Sand		$D_{50,r}/D_{50,s}$
	$D_{50,r}$ (mm)	Coefficient of uniformity $C_{u,r} = D_{60,r}/D_{10,r}$	$D_{50,s}$ (mm)	Coefficient of uniformity $C_{u,s} = D_{60,s}/D_{10,s}$	
Mixture 1	1.6	1.57	0.8	1.37	2
Mixture 2	1	2.02	0.2	2.22	5
Mixture 3	2	2.56	0.2	2.22	10

measured through direct shear testing of the mixtures, as shown in Fig. 2. The mixtures were subjected to three different vertical effective stress levels $\sigma'_v = 10$ kPa, 20 kPa and 30 kPa. These stress levels represent typical values of vertical effective stress on the foundation of low-cost, one-storey, housing/school solutions in developing countries [4,5]. Indicatively, to put things in context, $\sigma'_v = 30$ kPa corresponds to the foundation stress of a 4 × 4m, one storey masonry structure/room with a 0.2 m thick slab resting on 0.4 m thick, 3 m high reinforced or unreinforced masonry walls, while $\sigma'_v = 10$ kPa refers to a common design case in developing regions of a 6 × 8m classroom with a light steel roof supported by 2 m high, 0.4 m thick masonry walls through standard size tubular IPE steel columns. The foundation stress levels between the two structures vary mainly due to the difference between the weights of the concrete slab and the light steel roof, respectively.

The volume rubber fraction F_R in a sand-rubber mixture is defined as [26]:

$$F_R = \frac{V_R}{V_R + V_S} \tag{1}$$

where V_R is the volume of rubber in the mixture and V_S is the volume of sand in the mixture.

A rubber volume fraction equal to $F_R = 50\%$ was used for all the mixtures investigated in this study. This rubber fraction value was chosen to exceed the volume fraction threshold $F_R = 30\%$ for rubber-dominated behaviour of the sand-rubber mixture observed by Rouhanifar and Ibraim [26] and to facilitate an easy selection of the ingredients of the mixture, which is independent from the measuring equipment available in the construction site.

The grain size distribution of a sand-rubber mixture is another fundamental parameter that influences the behaviour of the mixture. The mean grain sizes and the coefficients of uniformity of rubber and sand that were used for the three different sand-rubber mixtures investigated in this study and the relative mean size ratios of each of the mixtures ($D_{50,r}/D_{50,s}$) are shown in Table 1. The grain sizes of the rubber particles were selected due to the attractive frictional characteristics of the sand-rubber samples consisting of these rubber grain sizes observed by Rouhanifar and Ibraim [26]. The rubber particles of these mixtures with Specific Gravity $G_r = 1.04$ were produced from shredded truck tyres and can be easily found in low income countries. Each rubber particle consists of polymer (56%), acetone (5–20%), carbon black (25–35%), ash (15%) and sulphur (1–3%) [24].

The two types of sand used in this study are: Leighton Buzzard sand (Mixture 1, $e_{max} = 0.84$, $e_{min} = 0.53$, Specific Gravity $G_S = 2.65$) [41] and Redhill sand (Mixtures 2 and 3, $e_{max} = 1.04$, $e_{min} = 0.61$, Specific Gravity $G_S = 2.65$) [43]. The preparation of each sand-rubber sample consisted of mixing of the particles of the two materials and dry deposition with zero-height drop using a funnel to a target initial void ratio of $e = 0.73$.

The friction of three different sand-rubber mixtures subjected to vertical stress $\sigma'_v = 10$ kPa, 20 kPa and 30 kPa against a timber (plywood) interface was measured through direct shear testing of the mixtures, as shown in Fig. 3.

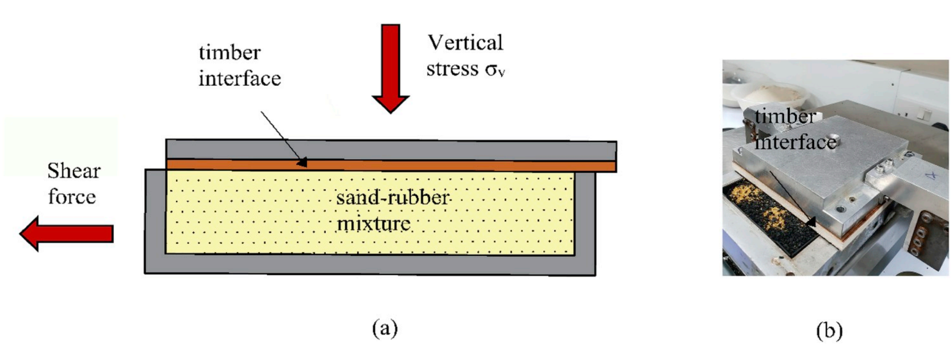

Fig. 3. (a) Schematic representation and (b) Picture of direct shear testing of the interface between timber and sand-rubber mixture.

3. Experimental results of direct shear testing of sand-rubber mixtures

3.1. Validation of the experimental procedure

The experimental process presented in Section 2 was followed for the determination of the shear stress-horizontal displacement curve of a sand-rubber mixture with $D_{50,r}/D_{50,s} = 2$ subjected to vertical stress $\sigma'_v = 30$ kPa using the conventional direct shear apparatus and the modified direct shear apparatus described by Lings and Dietz [41]. As shown in Fig. 4, the maximum shear stress values obtained using the modified direct shear apparatus were 15% lower than the ones obtained using the commonly used direct shear apparatus and were compared with the corresponding values derived by Anvari et al. [44] for the similar sand-rubber mixture and vertical stress conditions. The applied shear rate (SR) was 0.5 mm/min. The values shown in Fig. 4 were systematically observed after four repetitions of this test that showed a maximum difference of 10% from the presented results. This repeatability of the results obtained using the modified direct shear apparatus and their excellent agreement with the values derived by Anvari et al. [44] validated the experimental process presented in Section 2 and the use of the modified direct shear apparatus for the direct shear testing performed in this study.

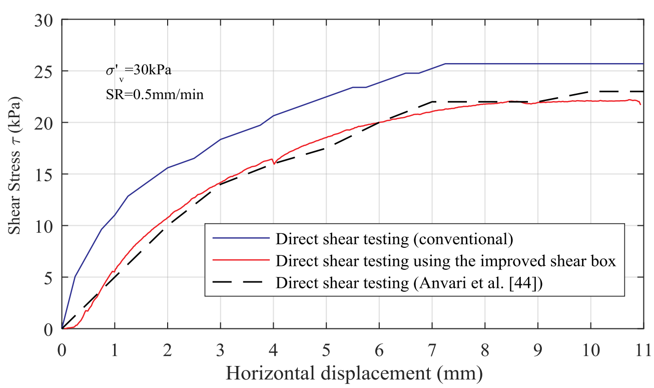

Fig. 4. Shear stress-horizontal displacement curve due to direct shear testing of a sand-rubber mixture with grain ratio $D_{50,r}/D_{50,s} = 2$ subjected to vertical stress $\sigma'_v = 30$ kPa using (a) The commonly used direct shear apparatus (b) The Lings and Dietz modified direct shear apparatus. Comparison with the shear stress-displacement results obtained by Anvari et al. [44] for the same sand-rubber mixture under the same vertical stress conditions.

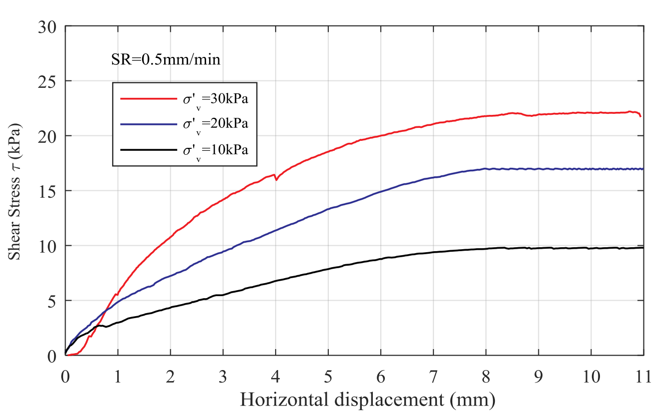

Fig. 5. Shear stress-horizontal displacement curve due to direct shear testing of a sand-rubber mixture with grain ratio $D_{50,r}/D_{50,s} = 2$ subjected to vertical stress $\sigma'_v = 30$ kPa, $\sigma'_v = 20$ kPa and $\sigma'_v = 10$ kPa using the Lings and Dietz modified direct shear apparatus.

The effect of the vertical stress on the presented results is illustrated in Fig. 5. As expected, the shear stress decreases for lower values of vertical stress. The observed sliding displacement at zero force for the case of $\sigma'_v = 30$ kPa for a horizontal displacement smaller than 0.25 mm is attributed to a deflection of the shear box due to improper fixity of the system at the beginning of the test.

3.2. Comparison with pure sand and pure rubber direct shear testing results

The beneficial role of a sand-rubber mixture towards the reduction of the friction angle comparing to a pure sand sample of the same material and grain size are illustrated in Fig. 6. The friction angle obtained in a sand-rubber mixture with $D_{50,r}/D_{50,s} = 2$ subjected to vertical stress $\sigma'_v = 30$ kPa is substantially lower than the one obtained from a sand mixture of the same properties for horizontal displacement values smaller than 5 mm.

This friction angle reduction is approximately 40% for a horizontal displacement value of 1 mm (Fig. 6) and indicates a delay in the interlocking between the sand particles in the mixture due to the presence of the rubber particles. However, the ultimate value of friction angle (at larger displacements) is 10% larger for the sand-rubber mixture than for the sand sample.

The presented friction angle of 20° for the sand-rubber mixture for a horizontal displacement of 1 mm corresponds to an angle of friction coefficient $\tan\varphi = 0.36$. The exceedance of this coefficient for an earthquake ground motion acceleration of 0.36 g could trigger a shear failure mechanism within this layer, thus facilitating the potential use of this mixture as a response modification strategy.

The attractive frictional characteristics of the presented sand-rubber mixture for low horizontal displacement values are confirmed for the case of cyclic direct shear testing shown in Fig. 7a. The normalization of the shear stress to the vertical stress τ/σ'_v of the mixture indicates the angle of friction coefficient $\tan\varphi$ of the mixture for varying horizontal displacement values. The applied shear rate (SR) was 0.75 mm/min.

Interesting conclusions are drawn by the comparison of the presented cyclic response of the sand-rubber mixture with a pure rubber sample of the same grain size. The cyclic response of both samples is investigated to account for the load reversal occurring during an earthquake event. In particular, the angle of friction coefficient obtained from the pure rubber sample is significantly lower than the one obtained from the use of a sand-rubber mixture. However, the vertical displacement of the pure rubber sample measured before the conduction of the direct shear testing due to a vertical stress of $\sigma'_v = 30$ kPa was two times higher than the corresponding vertical settlement of the sand-rubber mixture, as shown in Fig. 7b. This vertical settlement of the rubber mixture could lead to a significant vertical settlement of the

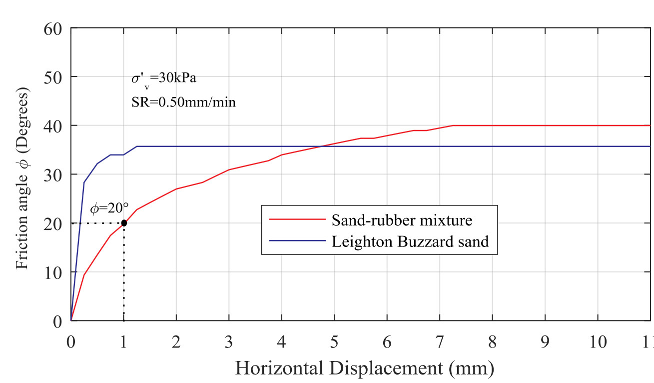

Fig. 6. Friction angle-horizontal displacement curve resulting from direct shear testing of a sand-rubber mixture with $D_{50,r}/D_{50,s} = 2$ and a Leighton Buzzard sand sample with $D_{50,s} = 0.8$ mm subjected to vertical stress $\sigma'_v = 30$ kPa.

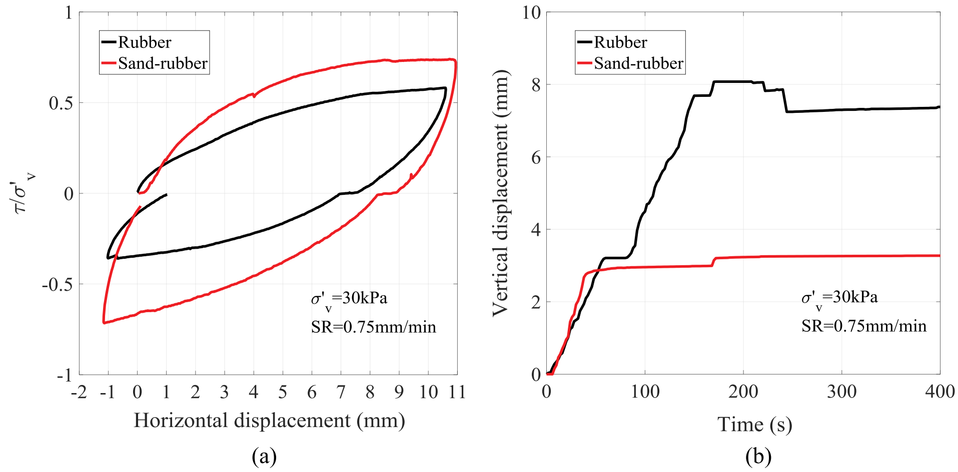

Fig. 7. (a) Normalized shear stress-horizontal displacement curve and (b) Vertical displacement time history of a sand-rubber mixture with $D_{50,r}/D_{50,s} = 2$ and a rubber sample with $D_{50,r} = 1.6$ mm subjected to vertical stress $\sigma'_v = 30$ kPa.

structure founded on this layer, which could inhibit the functionality of the structure, particularly if it is combined with tilting of the foundation slab.

Therefore, the choice of a sand-rubber layer as a seismic isolation strategy is a direct outcome of a favourable balance between low friction and the maintenance of vertical settlement within reasonable limits comparing to pure sand or a pure rubber layer design solutions.

3.3. Effect of shear rate and saturation on the direct shear testing of sand-rubber mixtures

The effect of shear rate on the normalized shear stress-horizontal displacement curve of a sand-rubber mixture with $D_{50,r}/D_{50,s} = 2$ subjected to vertical stress $\sigma'_v = 30$ kPa is shown in Fig. 8a. The angle of friction coefficient defined as the ratio of the shear stress τ over the vertical stress σ'_v decreases for shear rates increasing from $SR = 0.75$ mm/min to $SR = 1.25$ mm/min. This result indicates a tendency for a decrease of the angle of friction coefficient for higher shear velocities, which is the case in earthquake ground motion excitation. However, the shear velocities during a ground motion excitation are much higher and the presented results should be confirmed through dynamic testing.

The saturation of a sand-rubber mixture is another factor that influences its frictional characteristics significantly: Fig. 8b shows that the angle of friction coefficient obtained through a fully saturated sample with $D_{50,r}/D_{50,s} = 2$ subjected to vertical stress $\sigma'_v = 30$ kPa is 10% lower than the corresponding angle of friction coefficient obtained through a dry sample subjected to the same vertical stress levels.

The differences between dry and fully saturated laboratory specimens are attributed to the lubrication of the specimen due to the

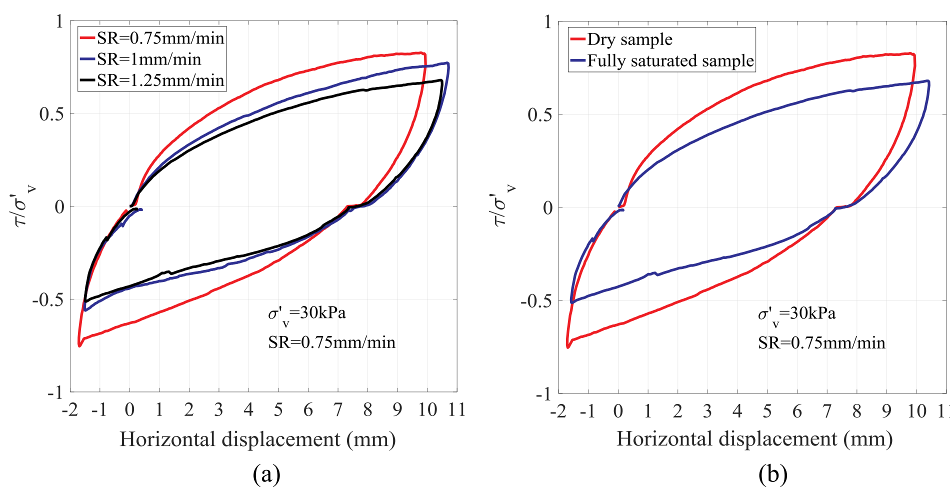

Fig. 8. Effect of (a) shear rate and (b) saturation on the normalized shear stress-horizontal displacement curve due to direct shear testing of a sand-rubber mixture with $D_{50,r}/D_{50,s} = 2$ subjected to vertical stress $\sigma'_v = 30$ kPa.

presence of water. The design implication of this result is the ability of a sand-rubber layer to maintain and even improve its frictional characteristics for fully saturated conditions corresponding to rain or high level of groundwater reaching the level of the sand-rubber mixture below the designed structure. However, the behaviour of the mixture for partially saturated conditions was not investigated in this study.

3.4. Effect of mean size ratio on direct shear testing of sand-rubber mixtures

The influence of the mean grain size ratio on the normalized shear stress-horizontal displacement curve of the three selected sand-rubber mixtures presented in Section 2 is shown in Fig. 9. The objective of this test is the comparison of the behaviour of mixtures with alternative grain sizes towards the selection of the sand-rubber layer with the optimal mechanical characteristics as a seismic isolation strategy for developing countries.

As shown in the figure, the use of a sand-rubber mixture with $D_{50,r}/D_{50,s} = 5$ leads to the minimal angle of friction coefficient τ/σ'_v of a potential failure mechanism inside a sand-rubber layer for large horizontal displacement values. The use of a sand-rubber mixture with $D_{50,r}/D_{50,s} = 2$ yields the highest angle of friction coefficient, among the investigated mixtures, while the friction obtained with a mixture of $D_{50,r}/D_{50,s} = 10$ lies between the other two aforementioned values. However, the difference in the response between the three mixtures for low horizontal displacement values is minimal.

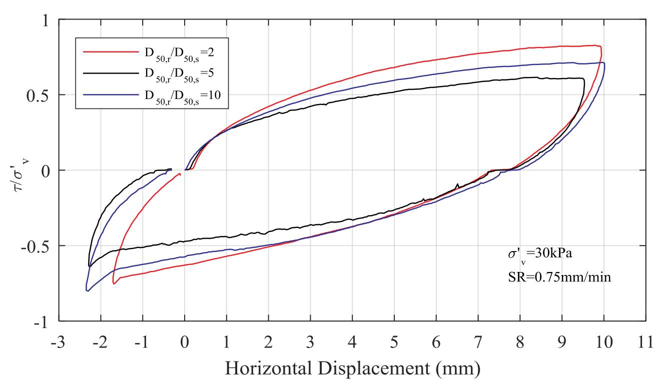

Fig. 9. Effect of mean size ratio on the normalized shear stress-horizontal displacement curve due to direct shear testing of three different sand-rubber mixtures subjected to vertical stress $\sigma'_v = 30$ kPa.

3.5. Direct shear testing of a timber sliding interface against a sand-rubber mixture

The normalized shear-stress-displacement curve of a sand-rubber mixture with $D_{50,r}/D_{50,s} = 5$ obtained from a direct-shear testing of the mixture against a timber sliding interface as presented in Section 2 is shown in Fig. 10. The objective of this test is the investigation of the sliding behaviour and the associated seismic isolation efficiency gained from the use of a timber sheet as a permanent formwork for the casting of a foundation slab of a structure based on a sand-rubber layer. The data obtained from this test and the previously shown direct shear tests illuminate two possible different failure mechanisms that can occur in the foundation of a structure based on a sand-rubber layer: A failure mechanism inside the sand-rubber layer and a sliding failure mechanism occurring in the surface between the interface and the sand-rubber layer.

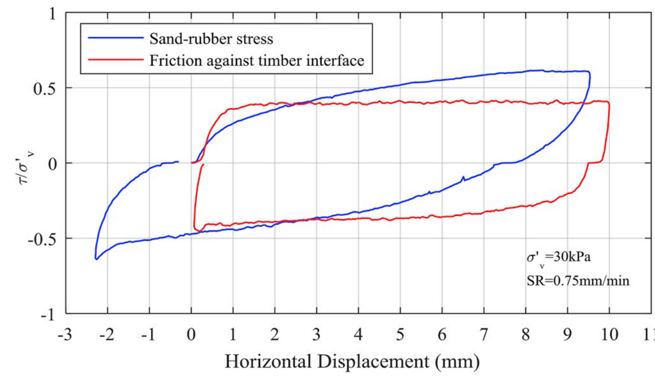

Fig. 10. Comparison of normalized shear stress-horizontal displacement curves derived from a) Direct shear testing of a sand-rubber mixture with $D_{50,r}/D_{50,s} = 5$ subjected to vertical stress $\sigma'_v = 30$ kPa and b) Direct shear testing of a sand-rubber mixture with $D_{50,r}/D_{50,s} = 5$ subjected to vertical stress $\sigma'_v = 30$ kPa against a timber sliding interface.

The obtained normalized stress curve yields a maximum static friction coefficient of $\mu_s = \tau/\sigma'_v = 0.4$ for this mixture and the selected timber sliding interface. The comparison of this curve with the results obtained from the direct shear testing of the same sand-rubber mixture for the same vertical stress indicates the sequence of the activation of the two different failure mechanisms occurring in the foundation of a structure based on a sand-rubber layer: A failure mechanism expressed by an angle of friction coefficient value that is lower than $\tan\varphi = \tau/\sigma'_v = 0.3$ is expected to occur first inside the sand-rubber layer for low displacement values before sliding occurs and then it is followed by sliding of the timber interface against the mixture for a static friction coefficient of $\mu_s = 0.4$.

The influence of the vertical stress on the presented results is presented in Fig. 11a. The decrease of the vertical stress from 30 kPa to 10 kPa does not have significant influence on the obtained friction coefficient. The favourable role of soil saturation on the frictional characteristics of a sand-rubber mixture with $D_{50,r}/D_{50,s} = 5$ against a timber sliding interface subjected to vertical stress $\sigma'_v = 30$ kPa is presented in Fig. 11b: The direct shear testing of a fully saturated sand-rubber mixture leads to a 20% decrease of the frictional strength comparing to the same dry sample, thus facilitating earlier sliding of a structure founded on a sand-rubber layer for saturated soil conditions.

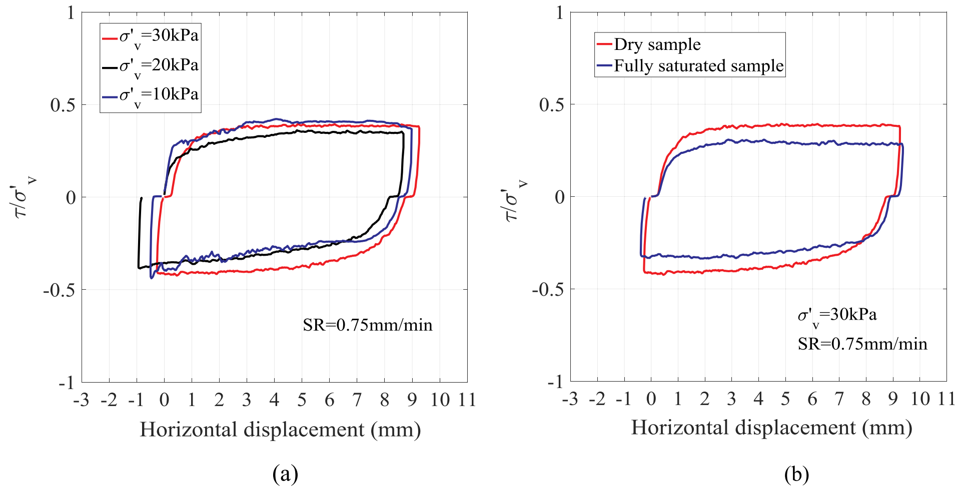

Fig. 11. Effect of (a) Vertical stress σ'_v and (b) Saturation on the normalized shear stress-horizontal displacement curve due to direct shear testing of a sand-rubber mixture with $D_{50,r}/D_{50,s} = 2$ against a timber sliding interface.

3.6. *Effect of mean size ratio on direct shear testing of sand-rubber mixtures against a timber sliding interface*

The influence of the mean grain size ratio on the normalized shear stress-horizontal displacement curves of the three selected sand-rubber mixtures presented in Section 2 against a timber sliding interface is shown in Fig. 12. The aim of this test is the comparative assessment of the behaviour of mixtures with alternative grain sizes aiming at the determination of the sand-rubber layer with the optimal mechanical characteristics as a seismic isolation strategy for developing countries.

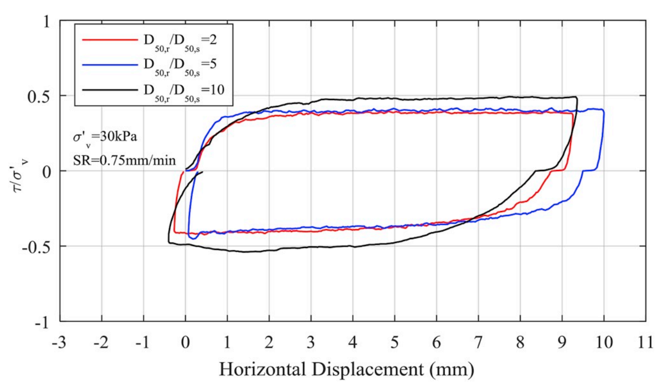

Fig. 12. Effect of mean size ratio on the normalized shear stress-horizontal displacement curve due to direct shear testing of a sand-rubber mixture with $D_{50,r}/D_{50,s} = 2$ against a timber sliding interface subjected to vertical stress $\sigma'_v = 30$ kPa.

As shown in the figure, the use of a sand-rubber mixture with $D_{50,r}/D_{50,s} = 2$ leads to the lowest (and for our purposes desirable) static friction coefficient $\mu_s = \tau/\sigma'_v = 0.38$ that triggers sliding of the timber interface against the sand-rubber mixture. A sand-rubber mixture with $D_{50,r}/D_{50,s} = 5$ manifests similar frictional behaviour with the mixture of $D_{50,r}/D_{50,s} = 2$ for large horizontal displacement values, but substantially higher friction expressed by $\mu_s = 0.44$ in the low displacement range. The use of a sand-rubber mixture with $D_{50,r}/D_{50,s} = 10$ yields the highest friction coefficient $\mu_s = 0.49$, among the investigated mixtures for large horizontal displacement values and similar frictional characteristics with the mixture of grain ratio $D_{50,r}/D_{50,s} = 2$ in the low displacement range. Henceforth, the choice of a sand-rubber mixture with grain ratio $D_{50,r}/D_{50,s} = 2$ emerges as the most attractive engineering solution towards the minimization of the static friction coefficient against a timber sliding interface, both in the low and the high horizontal displacement range.

4. Experimental procedure of dynamic shaking table testing

A uniaxial shaking table experimental setup shown in Figs. 13 and 14 was used for the investigation of the dynamics of a rigid sliding block and the quantification of the kinetic friction of different sliding interfaces against two different sand-rubber mixtures for two different sand-rubber layer heights. A Perspex box with transparent walls was constructed to facilitate the enclosure of a sand-rubber layer with two different heights: 2 cm and 5 cm, as shown in Fig. 13. The sand-rubber

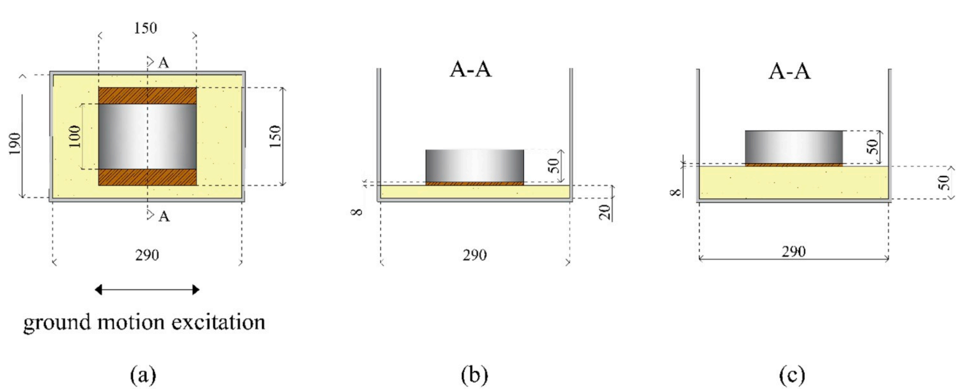

Fig. 13. (a) Overview and (b), (c) cross section of the experimental setup of a rigid steel structure based on a timber plate designed to slide against a sand-rubber layer of two different heights: 2 cm and 5 cm respectively.

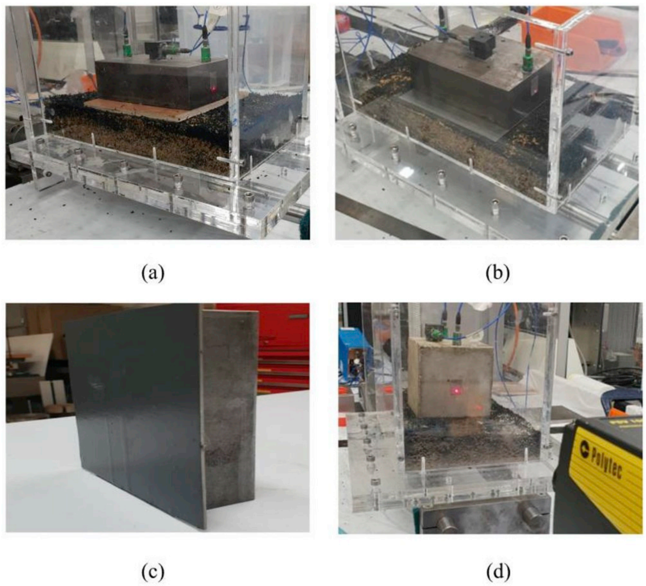

Fig. 14. Experimental setup of the sliding response of a rigid block on a sand-rubber layer using **a**) a steel block with a timber sliding interface **b**) a steel block with a steel sliding interface **c)** a steel block with a polythene sliding interface and **d)** a concrete block with a concrete sliding interface.

mixtures 1 and 2 presented in Section 2 (Table 1) were selected for this dynamic investigation, based on their attractive static frictional characteristics derived in Section 3 (Fig. 12).

A rigid steel block of dimensions 100 mmx150mm and height of 50 mm (Figs. 13 and 14a) was first based on a timber plate with dimensions 150 mmx150mm to quantify the kinetic frictional characteristics of a timber sliding interface against the aforementioned sand-rubber mixtures. The vertical stress acting on the sliding interface due to the weight of this block is $\sigma'_v = 3.9$ kPa. At a later stage of this investigation, the timber plate of the presented dimensions was replaced by a steel plate of the same dimensions to account for the effect of a steel sliding interface on the derived kinetic frictional characteristics (Fig. 14b). A polythene membrane of the same dimensions and thickness of 2 mm that is commonly used in developing countries was attached to the bottom surface of the steel plate to investigate the kinetic frictional characteristics of a polythene-sand-rubber sliding interface (Fig. 14c). The last part of this investigation consisted of the replacement of the rigid steel box by a concrete box with dimensions 100 mm × 100 mm and 80 mm height to consider the sliding response of a concrete surface against the presented sand-rubber mixtures, as shown in Fig. 14d.

The determination of parameter similitude laws between a small-scale experimental model and a real structure defined as the prototype is of utmost importance for the extrapolation of the conclusions of the experiment to the behaviour of real structures. The prototype structure in this study is a one storey 4 m × 6 m masonry classroom with a 0.2 m thick foundation slab and a light steel roof based on a sand-rubber layer. The fundamental design configuration of the foundation of the prototype structure based on the sand-rubber layer which is proposed in this study includes the use of a timber sheet as formwork for the casting of a concrete foundation slab. The use of timber is chosen due to the sustainability of the material and its availability in developing countries. This timber sheet is intended to remain attached below the concrete slab after casting, thus being used as the sliding interface between the structure and the sand-rubber layer. Therefore, the direct shear testing presented in this study focuses on the detailed investigation of the frictional characteristics of a timber interface against a sand-rubber layer. However, the scope of this study is expanded to four different sliding interfaces in the dynamic shaking table testing to investigate potential benefits from the use of these interfaces as design alternatives for the prototype structure.

Table 2
Dimensionless ratios and scaling factors used in dimensional analysis.

Dimensionless ratios to be maintained between the model and the prototype	Scaling factors between the model and the prototype
Acceleration ratio $\mu_s g/\alpha_g$	$\alpha_{g,\ model}/\alpha_{g,\ prototype} = 1$
Vibration period ratio T_s/T_g	$T_{g,\ model}/T_{g,\ prototype} = 0.85$

The weight of this structure corresponds to a foundation stress of 10 kPa. The foundation stress ratio of the prototype to the experimental model is 10kPa/3.9 kPa = 2.56. The mass ratio of the prototype to the experimental model is 25t/5.85 kg = 4273. The length ratio of the prototype to the experimental model is 40. Dimensional analysis was conducted in this study to establish the fundamental dimensionless parameters that govern the response of a structure founded on a sand-rubber layer, thus keeping the similitude between the structure and the prototype (Table 2): First, the dimensionless interface strength ratio $\mu_s g/\alpha_g$ (g is the acceleration of gravity). As shown in Fig. 11, the friction coefficient $\mu_s = \tau/\sigma'_v$ does not change significantly for varying vertical stress levels. Therefore, the acceleration amplitude of the excitation α_g should remain unchanged between the model and the prototype. Second, the dimensionless vibration period ratio of the isolated structure T_s over the period of the excitation T_g, where the period $T_s = 2\pi\sqrt{m/k}$ and the stiffness $k = \tau A/u$ (m is the mass of the rigid structure, τ is the shear stress, A is the area of the sliding interface and u is the horizontal displacement). The emerging scaling factors between the applied acceleration and excitation period in the model and the prototype structure are shown in Table 2.

The movement of the shaking table was controlled in displacement using a PID controller and the applied displacement was measured using a LVDT (Linear Variable Displacement Transducer). The acceleration of the shaking table was also monitored using an accelerometer. Simulink [45] and Dspace were used as an acquisition platform.

The sliding behaviour of the block was monitored by four sensors: three accelerometers, one measuring horizontal acceleration in the direction of the movement of the shaking table, the other two measuring the vertical acceleration components on its top corners (Fig. 14a,b,d). A laser velocity measurement sensor was used to extract the velocity and by integration the sliding displacement of the rigid block. The laser sensor pointed at a reflective tape attached to the rigid block, as shown in Fig. 14d. The advantage of using this laser sensor, as opposed to a LVDT sensor, for the sliding block displacement measures was that it was a non-contact measure which could not interfere with sliding.

5. Experimental results of dynamic shaking table testing

The experimentally derived acceleration response of a steel rigid block with a timber sliding interface (Figs. 13 and 14a) based on a sand-rubber layer of $D_{50,r}/D_{50,s} = 2$ with a height of 2 cm subjected to a harmonic ramp loading ground motion excitation is shown in Fig. 15. Preliminary results of this work can be found in the dissertation reports [46,47]. As shown in Fig. 15, the harmonic ground motion excitation of the rigid block with frequency varying from 2 to 10 Hz (frequency changing step = 1 Hz/s) led to a ramp-loading ground motion acceleration varying from 0.1 to 0.6 g. The horizontal axis of the figure refers to both time t in s and frequency f in Hz due to the chosen frequency changing step = 1 Hz/s. The harmonic ground motion acceleration input α_g (t) is given by Eq. (2) and (3):

$$a_g(t) = A(t)\sin(2\pi f(t)t) \tag{2}$$

where amplitude $A(t)$ is a staircase function, and frequency $f(t)$ is also defined as a staircase function:

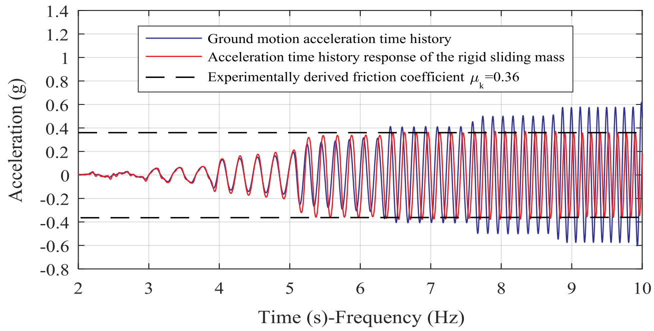

Fig. 15. Experimentally derived acceleration response of a steel rigid block with a timber sliding interface (Figs. 13 and 14a) based on a sand-rubber layer of $D_{50,r}/D_{50,s} = 2$ with a height of 2 cm subjected to harmonic ramp loading ground motion excitation.

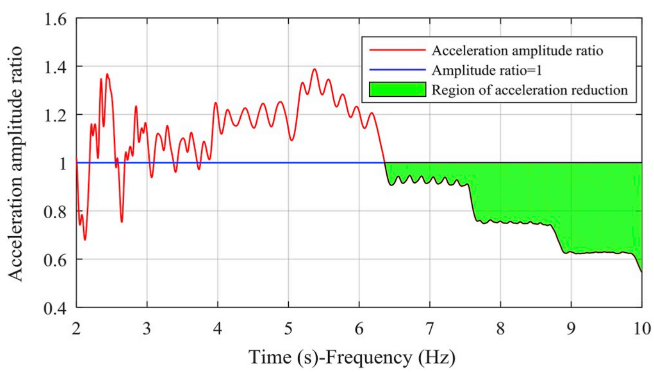

Fig. 16. Experimentally derived acceleration response amplitude ratio of a steel rigid block with a timber sliding interface (Figs. 13 and 14a) based on a sand-rubber layer of $D_{50,r}/D_{50,s} = 2$ with a height of 2 cm subjected to harmonic ramp loading ground motion excitation.

$$A(t) = 0.1g\sum_{j=1}^{10} H(t-j), \quad f(t) = 2 + \sum_{j=1}^{10} H(t-j) \tag{3}$$

where $H(t)$ is a Heaviside function.

The time history of the ratio of the acceleration response amplitude of the structure to the ground motion acceleration amplitude is presented in Fig. 16. The experimentally derived acceleration response of the sliding rigid block (Figs. 15 and 16) shed light to the different response modification phases of a rigid block sliding on a sand-rubber layer. First, a phase where the acceleration of the block is the same with the acceleration of the base (2–4 Hz). During this phase, the layer does not amplify the ground motion and there is no relative displacement between the block and the layer. Second, a phase where the acceleration of the block is higher than the acceleration of the layer (4 Hz–6Hz). During this phase, the sand-rubber layer amplifies the ground motion of the base by an average factor of 1.3 (Fig. 16), but there is still only minor relative displacement between the block and the layer. Even though this amplification corresponds to moderate intensity motions, further investigation through Finite Element Modelling or other research tools is required for the optimization of the thickness of the sand-rubber layer and the minimization of the amplification effect on the response of the structure founded on the sand-rubber layer. Third, a phase where the acceleration of the block is constant and significantly

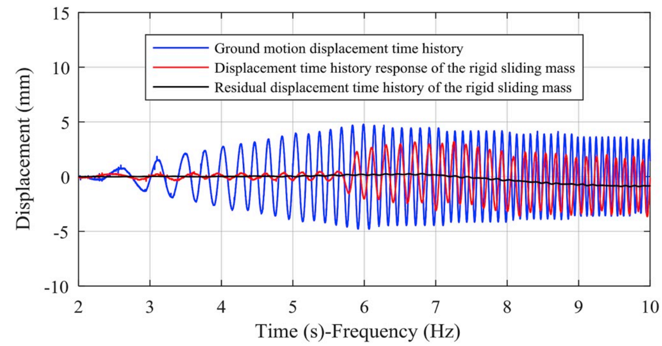

Fig. 17. Experimentally derived sliding displacement response of a steel rigid block with a timber sliding interface (Figs. 13 and 14a) based on a sand-rubber layer of $D_{50,r}/D_{50,s} = 2$ with a height of 2 cm subjected to harmonic ramp loading ground motion excitation.

smaller than the ground motion acceleration, which is the desired response. The region where the beneficial acceleration reduction occurs (acceleration ratio smaller than one) due to the seismic isolation effect of the proposed strategy is illuminated in Fig. 16. This phase is characterized by the sliding relative displacement of the rigid block with respect to the sand-rubber mixture, as shown in Fig. 17. The residual displacement of the rigid block with respect to the sand-rubber mixture is also presented on the same Figure. The experimentally derived acceleration threshold that corresponds to the initiation of this sliding behaviour defines the kinetic friction coefficient of the timber sliding interface against the selected sand-rubber mixture $\mu_k = 0.36$ (Fig. 15).

The increase of the acceleration amplitude in this shaking (Fig. 15) occurs simultaneously with the increase of the excitation frequency (Eq. (2) and (3)). Therefore, these figures illustrate a combination of acceleration amplitudes and frequencies, which trigger sliding of the rigid structure. The proximity of the selected ground motion frequencies in this excitation to realistic earthquake ground motion frequencies facilitates the extrapolation of the derived combination of acceleration and frequency values which trigger sliding behaviour to realistic structures subjected to earthquake ground motion excitation.

5.1. Effect of mean size ratio on the dynamic sliding response

The experimentally derived acceleration response of a steel rigid block with a timber sliding interface based on a sand-rubber layer of $D_{50,r}/D_{50,s} = 5$ with a height of 2 cm subjected to a harmonic ramp loading ground motion excitation is shown in Fig. 18. As shown in the figure, the experimentally derived kinetic friction coefficient (μ_k) of the timber sliding interface against the selected sand-rubber mixture is $\mu_k = 0.43$.

This kinetic friction value of $\mu_k = 0.43$ (for $D_{50,r}/D_{50,s} = 5$) is higher than the one obtained for the sand-rubber mixture with $D_{50,r}/D_{50,s} = 2$. However, this 15% increase of the kinetic friction coefficient of the timber sliding interface against the selected sand-rubber mixture is consistent with the increase of the corresponding static friction coefficient comparing to the sand-rubber mixture with $D_{50,r}/D_{50,s} = 2$ which was shown in Fig. 12 for low values of horizontal displacement, thus indicating that the sliding of the structure founded on the sand-rubber layer occurs mainly close to the interface between the foundation of the structure and the sand-rubber layer.

The initiation of sliding for the second mixture ($D_{50,r}/D_{50,s} = 2$) at

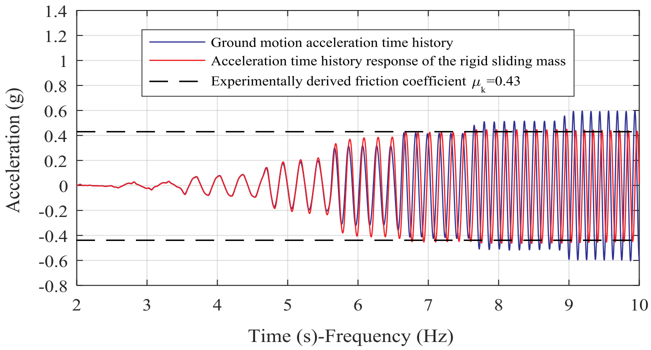

Fig. 18. Experimentally derived acceleration response of a steel rigid block with a timber sliding interface (Figs. 13 and 14a) based on a sand-rubber layer of $D_{50,r}/D_{50,s} = 5$ with a height of 2 cm subjected to harmonic ramp loading ground motion excitation.

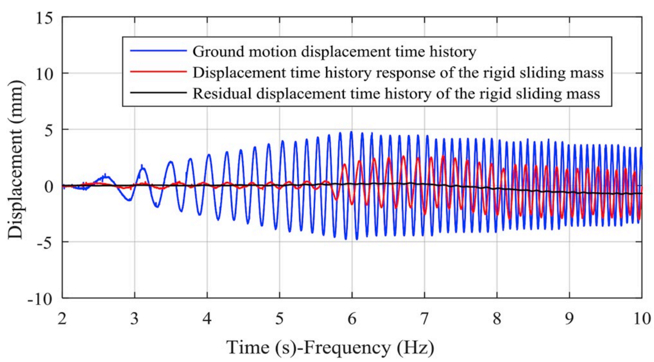

Fig. 19. Experimentally derived sliding displacement response of a steel rigid block with a timber sliding interface (Figs. 13 and 14a) based on a sand-rubber layer of $D_{50,r}/D_{50,s} = 5$ with a height of 2 cm subjected to harmonic ramp loading ground motion excitation.

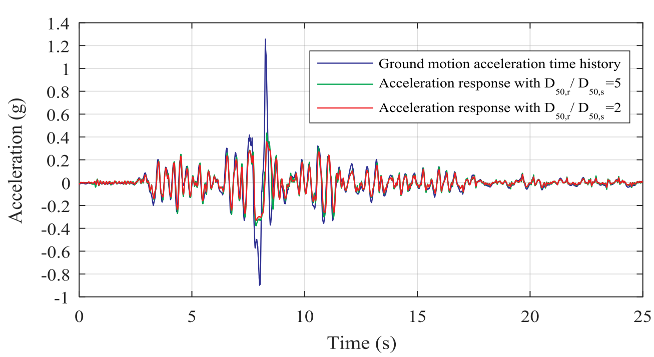

Fig. 20. Experimentally derived acceleration response of a steel rigid block with a timber sliding interface (Figs. 13 and 14a) based on two different sand-rubber layers of grain ratios $D_{50,r}/D_{50,s} = 5$ and $D_{50,r}/D_{50,s} = 2$ with a height of 2 cm subjected to Northridge ground motion excitation.

the aforementioned ground motion acceleration level occurring for a ground motion excitation frequency higher than 6 Hz is confirmed in Fig. 19: The relative sliding displacement of the rigid block with respect to the sand-rubber layer is shown for varying frequencies. Although the maximum acceleration of the rigid block is 0.43 g, there is an indication for initiation of soil deformation and/or sliding for a lower acceleration amplitude of 0.3 g. (Fig. 19). The residual displacement of the rigid block with respect to the sand-rubber mixture is also presented on Fig. 19.

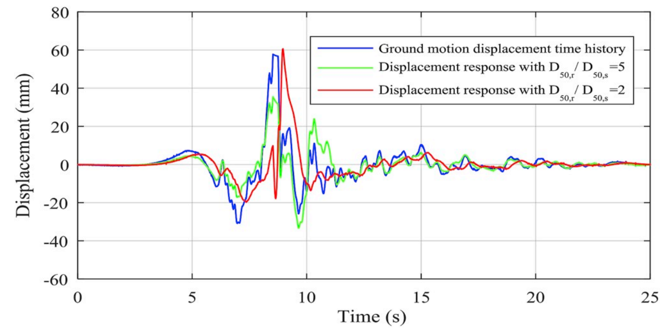

Fig. 21. Experimentally derived sliding displacement response of a steel rigid block with a timber sliding interface (Figs. 13 and 14a) based on two different sand-rubber layers of grain ratios $D_{50,r}/D_{50,s} = 5$ and $D_{50,r}/D_{50,s} = 2$ with a height of 2 cm subjected to Northridge ground motion excitation.

The acceleration and relative (with respect to the sand-rubber layer) sliding displacement response of the rigid block founded on the two different sand-rubber mixtures subjected to the 70%-scaled Northridge 1994 Tarzana (Record number 1087) ground motion excitation is shown in Figs. 20 and 21. The presented ground motion acceleration record was obtained from the PEER ground motion database [48].

As shown in Fig. 20, the kinetic friction coefficients derived by the ground motion acceleration level (g) at which the friction of the interface is exceeded and sliding occurs were consistent with the experimentally obtained values for harmonic ramp loading of both sand-rubber mixtures, namely $\mu_k = 0.36$ for $D_{50,r}/D_{50,s} = 2$ and $\mu_k = 0.43$ for $D_{50,r}/D_{50,s} = 5$. The maximum acceleration of the block observed for the two mixtures is 0.36 g and 0.43 g, respectively, thus validating the experimentally derived results for the harmonic ramp loading ground motion excitation. The maximum sliding displacement response of the rigid mass against the two different mixtures is 6 cm and 3.5 cm, respectively. This significant sliding displacement of the rigid mass is attributed to the long duration of the dominant pulse of the ground motion excitation, as shown in Figs. 20 and 21. Mylonakis and Voyagaki [49] and Voyagaki et al. [50] have investigated the effect of the shape and the duration of analytical pulse excitation on the response of sliding blocks on sliding interfaces, illustrating that the displacement demand of these structures increases significantly for increasing pulse duration. Tsiavos et al. [51] and Tsiavos and Stojadinovic [52] observed this high displacement demand in the response of stiff conventional and seismically isolated structures subjected to strong ground motion excitation.

5.2. Effect of height of sand-rubber layer on the dynamic sliding response

The influence of the height of the sand-rubber layer with $D_{50,r}/D_{50,s} = 2$ on the dynamic response of the presented rigid block with a timber sliding interface subjected to ramp loading ground motion excitation is shown in Fig. 22. The dynamic amplification in the acceleration response of the rigid block in the frequency range between 5 and 6 Hz before the initiation of sliding was higher for the sand-rubber layer with height $H = 5$ cm, comparing to the sand-rubber layer with height $H = 2$ cm. Additionally, the experimentally derived friction coefficient of the timber sliding interface against the sand-rubber layer with height $H = 5$ cm after sliding was $\mu_k = 0.46$, a value that is much higher than the corresponding value of $\mu_k = 0.36$, which was derived for the sand-rubber layer with height $H = 2$ cm (Fig. 15). As expected, the increase of the thickness of the layer increases the amplification since the layer becomes 'significant' with each own characteristics. At an excitation frequency of 6 Hz, the amplification factor is 2.0. Henceforth, the determination of the optimal height of the sand-rubber layer requires further study and optimization.

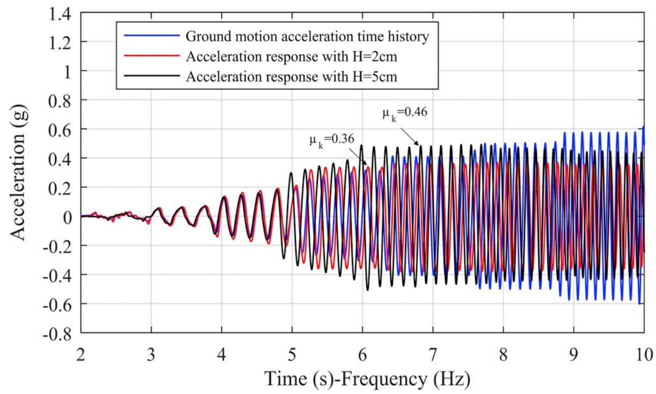

Fig. 22. Experimentally derived acceleration response of a steel rigid block with a timber sliding interface (Figs. 13 and 14a) based on a sand-rubber layer of $D_{50,r}/D_{50,s} = 2$ with two different heights $H = 2$ cm and $H = 5$ cm (Fig. 13) subjected to harmonic ramp loading ground motion excitation.

5.3. Effect of the material of the sliding-interface on the dynamic sliding response

The material of the sliding-interface is another fundamental design parameter that influences the dynamic response of a structure founded on a sand-rubber layer. Four different sliding interfaces consisting of four different materials (steel, timber, polythene, concrete) were investigated for the determination of potential differences in the sliding response of the presented rigid block based on a sand-rubber layer of $D_{50,r}/D_{50,s} = 2$ and $H = 2$ cm. The reason behind this investigation is the quantification of the effect of the material of the foundation slab of the structure founded on the sand-rubber layer on the sliding behaviour of the structure designed based on the proposed seismic isolation strategy for developing countries.

As shown in Fig. 23, there were only minor differences in the kinetic friction coefficients obtained for steel ($\mu_k = 0.34$), timber ($\mu_k = 0.36$) and polythene sliding interfaces ($\mu_k = 0.40$). However, the kinetic friction coefficient obtained for a concrete sliding interface ($\mu_k = 0.55$) was significantly higher. This result is expected: The proximity of the kinetic friction coefficient values obtained for a timber sliding interface ($\mu_k = 0.36$ for $D_{50,r}/D_{50,s} = 2$ and $\mu_k = 0.43$ for $D_{50,r}/D_{50,s} = 5$) through dynamic testing to the experimentally derived static friction coefficient values ($\mu_s = 0.38$ for $D_{50,r}/D_{50,s} = 2$ and $\mu_s = 0.44$ for $D_{50,r}/D_{50,s} = 5$) due to direct shear testing against a timber interface (Fig. 12) indicates that the fundamental mechanism that leads to the sliding response of a structure founded on a sand-rubber layer occurs close to the interface between the structure and the sand-rubber layer. However, three investigated materials manifested similar kinetic friction characteristics, thus leading to the following design outcome: A structure based on a timber, steel or polythene sliding interface that is designed to slide against the presented sand-rubber layer is expected to manifest similar sliding behaviour when subjected to strong ground motion excitation.

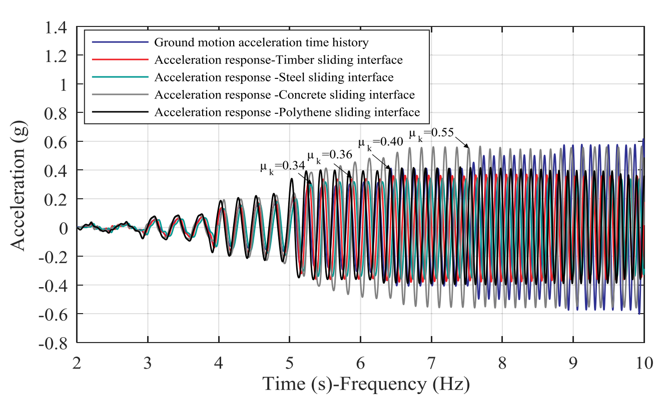

Fig. 23. Experimentally derived acceleration response of a rigid block with different sliding interfaces based on a sand-rubber layer of $D_{50,r}/D_{50,s} = 2$ with a height $H = 2$ cm subjected to harmonic ramp loading ground motion excitation.

6. Conclusions

An initial feasibility study towards the design of a new, low-cost, seismic isolation strategy for developing countries consisting of a sand-rubber foundation layer is presented in this paper. In contrast to previous studies addressing the static mechanical properties of materials or mixtures for seismic isolation purposes, this study presents a comprehensive static and dynamic experimental investigation of a wide spectrum of mechanical and geometrical properties of a deformable, granular sand-rubber layer, which can be used as a low-cost seismic isolation strategy in regions with limited material and financial resources.

Direct shear testing is performed to quantify the optimal grain size ratio of a sand-rubber mixture towards the minimization of friction and the facilitation of sliding against a timber interface. The choice of a sand-rubber mixture with $D_{50,r}/D_{50,s} = 2$ emerges as a more attractive engineering solution towards the minimization of the static friction coefficient against a timber sliding interface, both in the low and the high horizontal displacement range compared to the other two investigated mean grain size ratios of $D_{50,r}/D_{50,s} = 5$ and $D_{50,r}/D_{50,s} = 10$.

A uniaxial shaking table experimental setup is used for the investigation of the dynamics of a rigid sliding block and the quantification of the kinetic friction of different sliding interfaces against two different sand-rubber mixtures of two different layer heights. The choice of a sand-rubber mixture with $D_{50,r}/D_{50,s} = 2$ was found to minimize the kinetic friction coefficient against a timber sliding interface, thus facilitating sliding of a structure subjected to strong ground motion excitation. The excellent agreement between the frictional characteristics obtained from the dynamic shaking table tests and the direct shear tests of a timber interface against a sand-rubber mixture illuminated that the fundamental failure mechanism that triggers the sliding response of these structures is close to the interface between the foundation of the structure and the sand-rubber layer. Moreover, the conclusions obtained from both sets of tests confirmed the necessity for a hybrid static and dynamic approach for the assessment of the sliding behaviour of structures based on soil mixtures, which was not addressed in previous studies evaluating seismic isolation concepts for developing countries.

A sand-rubber layer height of 2 cm, which would correspond to a sand-rubber layer height of 80 cm in a 40 times-scaled-up realistic structure, was found to yield a more pronounced sliding behaviour for the structure compared to the other investigated sand-rubber layer height of 5 cm. Nevertheless, the determination of the optimal thickness of the sand-rubber layer requires further investigation using finite element modelling or other research tools. The use of a steel, a timber and a polythene sliding interface led to similar kinetic frictional characteristics against the presented sand-rubber layer, thus showing the applicability of the proposed seismic isolation strategy to a wide range of material design options defined by the local availability and the established building practices in each country.

However, the sliding surface alone is not assumed to be the only mitigation mechanism proposed in this study: The structure founded on the sand-rubber layer should be designed to withstand the inertial forces that correspond to the critical earthquake ground motion acceleration before sliding occurs. Along these lines, the design strategy which is proposed in this study for seismic damage mitigation in developing countries consists of three different behaviour ranges dependent on the earthquake ground motion intensity: For small intensity motions, sliding is not activated and the superstructure is designed to resist the seismic forces with simple and low-cost measures such as steel ties. For moderate intensity motions ($0.15\,g < PGA < 0.4\,g$), the foundation will shear within the soil rubber layer. For higher intensities exceeding the observed static friction coefficient of 0.4 ($PGA > 0.4\,g$), sliding is expected to occur between the sand-rubber layer and the timber formwork, thus reducing the seismic response and the associated seismic damage of the structure founded on the sand-rubber layer.

The presented experimental investigation will be followed by a set of large-scale experiments to be performed at the $3\,m \times 3\,m$ shaking table of University of Bristol, aiming for the investigation of the seismic sliding behaviour of steel and masonry structures founded on a sand-rubber layer using the design recommendations obtained in this study. This investigation will ultimately lead to the proposal of a complete, low-cost design solution for seismic damage mitigation in developing countries, consisting of materials that are locally available in these countries.

Data availability statement

The data to reproduce Fig. 4-12 and 15-23– be obtained from Ref. [53].

Acknowledgements

This work was supported by the EPSRC-funded research project 'SAFER' (Seismic Safety and Resilience of Schools in Nepal, EP/P028926/1). Prof. George Mylonakis is gratefully acknowledged for his valuable advice on the dimensional analysis performed in this study. The authors would like to thank Mr. Gary Martin, Mr. Adrian Kraft and the students Ms. Kate Conway and Mr. Billy Walkinshaw for their assistance during the conduction of the experimental work of this study in the Geomechanics Lab and the Dynamics Lab of University of Bristol.

References

[1] Kelly JM. A seismic base isolation: review and bibliography. Soil Dynam Earthq Eng 1986;5(3):202–16.
[2] Buckle IG, Mayes RL. Seismic isolation history, application and performance—a world view. Earthq Spectra 1990;6(2):161–201.
[3] Constantinou MC, Whittaker AS, Kalpakidis Y, Fenz DM, Warn GP. Performance of seismic isolation hardware under service and seismic loading Technical Report MCEER-07-0012 2007.
[4] United Nations. Standard country or area codes for statistical use. Series M, No. 49, rev. 4 (united nations publication, sales No. M.98.XVII.9) Available in part at http://unstats.un.org/unsd/methods/m49/m49regin.htm.
[5] OECD List of Developing Countries or Territories. Water Int 1997;22:1. https://doi.org/10.1080/02508069708686671.
[6] Kelly JM. Seismic isolation systems for developing countries. EERI Distinguished Lecture 2001. Earthquake Spectra 2002;18(3):385–406.
[7] Kelly JM, Konstantinidis D. Effect of friction on unbonded elastomeric bearings. J Eng Mech 2009;135(9):953–60.
[8] Castaldo P, Ripani M. Optimal design of friction pendulum system properties for isolated structures considering different soil conditions. Soil Dynam Earthq Eng 2018;90:74–87.
[9] Banović I, Radnić J, Grgić N. Geotechnical seismic isolation system based on sliding mechanism using stone pebble layer: shake-table experiments. Shock Vib 2019:26. Article ID 9346232 https://doi.org/10.1155/2019/9346232.
[10] Trifunac MD, Todorovska MI. Nonlinear soil response as a natural passive isolation mechanism—the 1994 Northridge, California earthquake. Soil Dynam Earthq Eng 1998;17(1):41–51.
[11] Trifunac MD. Nonlinear soil response as a natural passive isolation mechanism. Paper II. The 1933, Long Beach, California earthquake. Soil Dynam Earthq Eng 2003;23(7):549–62.
[12] Gazetas G, Anastasopoulos I, Adamidis O, Kontoroupi T. Nonlinear rocking stiffness of foundations. Soil Dynam Earthq Eng 2013;47:83–91.
[13] Anastasopoulos I, Kontoroupi TH. Simplified approximate method for analysis of rocking systems accounting for soil inelasticity and foundation uplifting. Soil Dynam Earthq Eng 2014;56:28–43.
[14] ASTM D6270 − 17. Standard practice for use of scrap tires in civil engineering applications. ASTM International; 2017.
[15] Ahmed I. Laboratory study on properties of rubber-soils. Joint highway research project. Purdue University, Indiana Department of Transportation; 1993.
[16] Tweedie J, Humphrey D, Sandford T. Tire shreds as lightweight retaining wall backfill: active conditions. J Geotech Geoenviron Eng 1998;124(11):1061–70.
[17] Hazarika H. Structural stability and flexibility during earthquakes using tyres (SAFETY)-A novel application for seismic disaster mitigation. Proceedings of the international workshop on scrap tire derived geomaterial-opportunities and challenges. Japan: Yokosuka; 2007.
[18] Hazarika H, Yasuhara K, Kikuchi Y, Karmokar AK, Mitarai Y. Multifaceted potentials of tire-derived three-dimensional geosynthetics in geotechnical applications and their evaluation. Geotext Geomembranes 2010;28(3):303–15.
[19] Edil TB, Bosscher PJ. Engineering properties of tire chips and soil mixtures. Geotech Test J 1994;17(4):453–64.
[20] Masad E, Taha R, Ho C, Papagiannakis T. Engineering properties of tire/soil mixtures as a lightweight fill material. Geotech Test J 1996;19(3):297–304.
[21] Foose GJ, Benson CH, Bosscher PJ. Sand reinforced with shredded waste tires. J Geotechn Eng (ASCE) 1996;122(9):760–7.
[22] Lee JS, Dodds J, Santamarina JC. Behavior of rigid-soft particle mixtures. J Mater Civ Eng 2007;19(2):179–84.
[23] Kim HK, Santamarina JC. Sand-rubber mixtures (large rubber chips). Can Geotech J 2008;45(10):1457–66.
[24] Lopera Perez JC, Kwok CY, Senetakis K. Effect of rubber content on the unstable behaviour of sand-rubber mixtures under static loading: a micro-mechanical study. Geotechnique 2018;68(7):561–74https://doi.org/10.1680/jgeot.16.P.149.
[25] Lopera Perez JC, Kwok CY, Senetakis K. Micromechanical analyses of the effect of rubber size and content on sand-rubber mixtures at the critical state. Geotext Geomembranes 2017;45(2):81–97.
[26] Rouhanifar S, Ibraim E. Laboratory investigation on the mechanics of soft-rigid soil mixtures. Deformation characteristics of geomaterials: 6th international symposium on deformation characteristics of geomaterials. Adv Soil Mech GeotechEng 2015;6:1073–80.
[27] Feng Z-Y, Sutter K. Dynamic properties of granulated rubber/sand mixtures. Geotech Test J 2000;23(3):338–44.
[28] Senetakis K, Anastasiadis A, Pitilakis K. Dynamic properties of dry sand/rubber (RSM) and gravel/rubber (GRM) mixtures in a wide range of shearing strain amplitudes. Soil Dynam Earthq Eng 2012;33:38–53.
[29] Uchimura T, Chi N, Nirmalan S, Sato T, Meidani M, Towhata I. Shaking table tests on effect of tire chips and sand mixture in increasing liquefaction resistance and mitigating uplift of pipe. In: Hazarika Yasuhara, editor. 23–24 March 2007, Yokosuka, Japan Proceedings of the international workshop on scrap tire derived geomaterials—opportunities and challenges. London: Taylor & Francis Group; 2007. p. 179–86.
[30] Hyodo M, Yamada S, Orense R, Okamoto M, Hazarika H. Undrained cyclic shear properties of tire chip-sand mixtures. In: Hazarika Yasuhara, editor. 23–24 March 2007, Yokosuka, Japan Proceedings of the international workshop on scrap tire derived geomaterials—opportunities and challenges. London: Taylor & Francis Group; 2007. p. 87–96.
[31] Anastasiadis A, Senetakis K, Pitilakis K. Small-strain shear modulus and damping ratio of sand–rubber and gravel–rubber mixtures. Geotech Geol Eng 2012;30(2):363–82.
[32] Tsang HH. Seismic isolation by rubber–soil mixtures for developing countries. Earthq Eng Struct Dyn 2008;37:283–303.
[33] Tsang HH, Lo SH, Xu X, Sheikh MN. Seismic isolation for low-to-medium-rise buildings using granulated rubber–soil mixtures: numerical study. Earthq Eng Struct Dyn 2012;41:2009–24.
[34] Mavronicola E, Komodromos P, Charmpis D. Numerical investigation of potential usage of rubber–soil mixtures as a distributed seismic isolation approach. Proceedings of the tenth international conference on computational structures technology 2010. Stirlingshire, UK: Civil-Comp Press.
[35] Brunet S, de la Llera JC, Kausel E. Non-linear modeling of seismic isolation systems made of recycled tire-rubber. Soil Dynam Earthq Eng 2016;85:134–45.
[36] Pitilakis K, Karapetrou S, Tsagdi K. Numerical investigation of the seismic response of RC buildings on soil replaced with rubber–sand mixtures. Soil Dynam Earthq Eng 2015;79:237–52.
[37] Tsang HH, Pitilakis K. Mechanism of geotechnical seismic isolation system: analytical modeling. Soil Dynam Earthq Eng 2019;122:171–84.
[38] Tsang HH. Geotechnical seismic isolation. Earthquake engineering: new research. New York: U.S. Nova Science Publishers Inc; 2009. p. 55–87.
[39] Jewell RA, Wroth CP. Direct shear tests on reinforced sand. Geotechnique 1987;37(1):53–68.
[40] Shibuya S, Mitachi T, Tamate S. Interpretation of direct shear box testing of sands as quasi-simple shear. Geotechnique 1997;47(4):769–90.
[41] Lings ML, Dietz MS. An improved direct shear apparatus for sand. Geotechnique 2004;4:245–56.
[42] O'Rourke TD. Geohazards and large, geographically distributed systems. Geotechnique 2010;60(7):505–43.
[43] Lombardi D, Bhattacharya S, Hyodo M, Kaneko T. Undrained behaviour of two silica sands and practical implications for modelling SSI in liquefiable soils. Soil Dynam Earthq Eng 2014;66:293–304.
[44] Anvari SM, Shooshpasha I, Kutanaei SS. Effect of granulated rubber on shear strength of fine-grained sand. Journal of Rock Mechanics and Geotechnical Engineering 2017;9(5):936–44.
[45] MATLAB and statistics toolbox release. Natick: The Mathworks Inc.; 2012.
[46] Conway KE. An experimental investigation into the influence of the sliding interface and grain size distribution on the dynamic sliding response of a small-scale structure. Undergraduate research report No 1819RP042 Bristol, UK: Department of Civil Engineering, University of Bristol; 2019. [Research project supervised by Dr. Nick Alexander and Dr. Anastasios Tsiavos)].
[47] Walkinshaw W. Experimental investigation into the significance of depth and particle size distribution of an isolation foundation on the sliding and rocking behaviour of a small-scale structure. Undergraduate Research Report No. 1819RP043 Bristol, UK: Department of Civil Engineering, University of Bristol; 2019. [Research

project supervised by Dr. Nick Alexander and Dr. Anastasios Tsiavos)].
[48] PEER NGA Strong Motion Database. Pacific earthquake engineering research center, University of California, Berkeley Accessed 08 October 2018 https://ngawest2.berkeley.edu/.
[49] Mylonakis G, Voyagaki E. Yielding oscillator subjected to simple pulse waveforms: numerical analysis and closed-form solutions. Earthq Eng Struct Dyn 2006;35(15):1949–74.
[50] Voyagaki E, Mylonakis G, Psycharis I. Rigid block sliding to idealized acceleration pulses. J Eng Mech 2012;138:1071–83.
[51] Tsiavos A, Mackie KR, Vassiliou MF, Stojadinovic B. Dynamics of inelastic base-isolated structures subjected to recorded ground motions. Bull Earthq Eng 2017;15(4):1807–30.
[52] Tsiavos A, Stojadinovic B. Constant yield displacement procedure for seismic evaluation of existing structures. Bull Earthq Eng 2018;17(4):2137–64.
[53] Tsiavos A. Supporting data for 'A sand-rubber deformable granular layer as a low-cost seismic isolation strategy in developing countries: experimental investigation'. https://doi.org/10.5523/bris.8ssqb7nd5whs2qkdt01b2dh58; 2019.